Knoblauch, C., Beer, C., Liebner, S., Grigoriev, M. N., Pfeiffer, E.-M. (2018): Methane production as key to the greenhouse gas budget of thawing permafrost. - *Nature Climate Change*, *8*, pp. 309—312.

DOI: http://doi.org/10.1038/s41558-018-0095-z

# Methane production as key to the greenhouse gas budget of thawing permafrost

Christian Knoblauch[1, 2*], Christian Beer[3, 4], Susanne Liebner[5], Mikhail N. Grigoriev[6], Eva-Maria Pfeiffer[1, 2]

[1]Institute of Soil Science, Universität Hamburg, Hamburg, Germany

[2]Center for Earth System Research and Sustainability, Universität Hamburg, Hamburg, Germany

[3]Department of Environmental Science and Analytical Chemistry, Stockholm University, Stockholm, Sweden

[4]Bolin Centre for Climate Research, Stockholm University, Stockholm, Sweden

[5]GFZ German Research Centre for Geosciences, Section Geomicrobiology, Potsdam, Germany

[6]Russian Academy of Sciences, Siberian Branch, Mel'nikov Permafrost Institute, Yakutsk, Russia

**Permafrost thaw liberates frozen organic carbon, which is decomposed to carbon dioxide ($CO_2$) and methane ($CH_4$). The release of these greenhouse gases (GHGs) forms a positive feedback to atmospheric $CO_2$ and $CH_4$ concentrations and accelerates climate change[1, 2]. Current studies report a minor importance of $CH_4$ production in water-saturated (anoxic) permafrost soils[3, 4, 5, 6] and a stronger permafrost carbon-climate feedback from drained (oxic) soils[1, 7]. Here we show through 7-year laboratory incubations that equal amounts of $CO_2$ and $CH_4$ are formed in thawing permafrost under anoxic conditions after stabile $CH_4$-producing microbial communities have established. Less permafrost carbon was mineralized under anoxic conditions but more $CO_2$-C equivalents were formed than under oxic conditions when taking the higher global warming potential (GWP) of $CH_4$ into account[8]. An organic carbon decomposition model, calibrated with the observed decomposition data, predicts until 2100 a higher loss of permafrost carbon under oxic conditions (113±58 g $CO_2$-C $kgC^{-1}$) but a twice as high production of $CO_2$-C equivalents (241±138 g $CO_2$-C-eq. $kgC^{-1}$) under anoxic conditions. These findings challenge the view of a stronger permafrost carbon-climate feedback from drained soils[1, 7] and emphasize the importance of $CH_4$ production in thawing permafrost on climate relevant time scales.**

Permafrost-affected landscapes of the northern hemisphere contain about 1300 Pg organic carbon of which about 800 Pg are perennially frozen in permafrost[9]. The predicted thawing of permafrost[1] will cause the microbial decomposition of this currently frozen organic carbon. In drained, oxic soils, microorganisms oxidize organic carbon to $CO_2$. Anoxic conditions, which prevail in water-saturated soils, slow down organic carbon decomposition[7] but enable the formation of both $CO_2$ and $CH_4$, latter having at least a 28 fold GWP of $CO_2$ (100 years)[8]. Since permafrost impedes water drainage, water-saturated soils are widespread in permafrost-affected landscapes though landscape hydrology will likely change in response to permafrost thawing[10, 11]. However, a major knowledge gap today concerns the dynamics of long-term anoxic organic carbon mineralization from thawing permafrost[12], which prevents a reliable projection of future land-atmosphere GHG exchange in northern permafrost areas.

While field observations demonstrate rising $CH_4$ emissions with soil warming and increased permafrost thaw[13, 14], laboratory incubations indicate that $CH_4$ represents only a minor fraction of total anoxic organic carbon decomposition in thawing permafrost[3, 4, 5, 6]. Therefore, current evidence suggests that permafrost thaw in dry soils will cause a stronger permafrost carbon-climate feedback than in water-saturated soils[1, 7]. However, anoxic incubation studies of permafrost are scarce and generally last for only several days to weeks[4, 5, 6]. Consequently, the role of $CH_4$ production on climate-relevant time scales is still highly uncertain.

We challenged the existing view that $CH_4$ production is of minor importance for organic carbon decomposition in thawing permafrost by two hypotheses. (H1) The reported low contribution of $CH_4$ production to anoxic carbon decomposition in thawing permafrost is due to the lack of an active methanogen community that only establishes over longer time periods. (H2) Long-term anoxic permafrost organic matter decomposition releases less carbon but more $CO_2$-C equivalents than oxic organic matter decomposition when considering the higher GWP of $CH_4$.

56 To test these hypotheses, we combined long-term incubation studies (> 7 years) of
57 permafrost samples with numerical modelling and simulated both oxic and anoxic GHG
58 production from thawing permafrost until 2100. Permafrost samples (n=29) from two sites in
59 northeast Siberia (Holozene river deposits, Pleistocene Yedoma sediments) were incubated
60 under oxic and anoxic conditions at 4 °C (ref 15). Samples were pre-incubated for four years
61 until constant $CH_4$ production rates were recorded in most of the anoxic samples before the
62 start of the main experiment spanning another three years (Suppl. Fig. S1).

63 Maximum $CO_2$ production rates were observed both under oxic and anoxic conditions at the
64 beginning of the pre-incubation phase[15] but anoxic $CH_4$ production only started after a lag-
65 phase lasting from few weeks up to several years. The multi-annual lag-phases indicate a
66 low abundance of methanogenic communities in the original samples, which may be caused
67 by permafrost formation under conditions not suitable for methanogenesis, e.g. in dry soils[16,
68 17]. However, these communities were activated after suitable conditions prevailed for long
69 enough time. Only four samples showed no $CH_4$ production even after seven incubation
70 years (Suppl. Table S1). The gene-copy numbers of the key enzyme of methanogenic
71 archaea (mcrA) were below the detection limit in these four samples (Suppl. Table S2).
72 When inoculating these inactive samples with permafrost material containing active
73 methanogens, $CH_4$ production could be established instantaneously in most samples (Fig. 1,
74 Suppl. Table S2). Hence, the lack in $CH_4$ production in these samples was caused by the
75 absence of methanogens and not by the intrinsic properties of permafrost organic matter.

76 After the pre-incubation phase of four years, representative samples (n=12, organic carbon
77 content of 0.6% to 12.4%, Suppl. Table S1) that passed maximum $CH_4$ production rates were
78 selected for the main experiment (Methods, Suppl. Fig. S1). Maximum $CH_4$ production rates
79 in these samples (mean = 4.9 ± 3.1 g $CH_4$-C $kgC^{-1}$ $yr^{-1}$, Suppl. Table S1) were four times
80 higher than maximum rates (1.2 g $CH_4$-C $kgC^{-1}$ $yr^{-1}$) from mainly short-term incubation
81 studies of pan-Arctic soils[12]. Under field conditions, permafrost thaw enables the exchange of
82 labile organic matter between the active layer and the former permafrost, e.g. by

cryoturbation[18] or leaching of DOC[19]. To simulate the input of fresh plant litter into thawing permafrost, the organic carbon mineralized during the pre-incubation phase was backfilled at the onset of the main experiment with $^{13}C$-labelled carbon from *Carex aquatilis*. Greenhouse gas production from permafrost carbon was quantified over another three years by the amount and the $\delta^{13}C$-signature of produced $CO_2$ and $CH_4$ (see Methods). Only GHG production from permafrost carbon, excluding GHG production from *Carex* carbon, was then used to calibrate a two-pool organic carbon decomposition model that was fitted to the non-linear decomposition of permafrost carbon over time (Fig. 2). After calibration, the model was run forward for each sample until 2100 (see Methods).

At the onset of the main experiment, $CO_2$ and $CH_4$ production rates from permafrost organic carbon were generally slightly higher than at the end of the pre-incubation phase, which might be due to the availability of fresh *Carex* litter causing a positive "priming" of permafrost organic carbon decomposition. However, this "priming effect" only lasted for about one month and caused a minor increase of permafrost organic carbon decomposition (Suppl. Text and Suppl. Table S3). Organic carbon decomposition rates further declined over the incubation period, which was most likely caused by the decreasing availability of labile organic components. During the three incubation years of the main experiment a mean amount of 19 ± 9.6 g $CO_2$-C $kg^{-1}$ of permafrost carbon (n=12) was mineralized to $CO_2$ under oxic conditions (Suppl. Table S4). Anoxic conditions slowed down organic carbon mineralization by a factor of 3.0 ± 1.2 (n=12, Suppl. Table S4) which confirms the ratio (3.4) previously reported as the mean for permafrost affected soils[7]. But more importantly, a similar amount of permafrost carbon was mineralized to $CO_2$ (3.2 ± 1.7 g $CO_2$-C $kgC^{-1}$, n=12) and to $CH_4$ (3.6 ± 1.9 g $CH_4$-C $kgC^{-1}$, n=12). When considering the higher GWP of $CH_4$, the average production of $CO_2$-C equivalents under anoxic conditions (40 ± 21 g $CO_2$-C equivalents $kgC^{-1}$, Suppl. Table S4) was about twice as high as under oxic conditions. The $CO_2$:$CH_4$ ratio for anaerobic organic carbon decomposition depends on the oxidation state of the organic carbon and the availability of alternative electron acceptors such as nitrate, ferric iron or sulfate, but under optimum conditions for methanogenesis about equal amounts of $CH_4$ and $CO_2$ are formed[20,

111 [21]. The $CO_2$:$CH_4$ ratio of 0.92 ± 0.18 (n=12, Fig. 2b insert, Suppl. Table S4) from the long-
112 term incubations is close to the theoretical value of about one, but three orders of
113 magnitudes lower than the ratio reported for permafrost samples (median = 1163) in a meta-
114 analysis of mainly short-term incubations[12]. Our results indicate an equal contribution of $CO_2$
115 and $CH_4$ production during anaerobic decomposition of permafrost organic carbon as soon
116 as an active methanogen community has established (H1).

117 Available field observations consistently show $CH_4$ production in the active layer of water
118 saturated permafrost soils[13, 22, 23, 24] and indicate elevated $CH_4$ emissions after permafrost
119 thaw as long as water saturated conditions prevail[13, 14, 22]. Therefore, it is unclear if the
120 observed long lag-phase is also required for establishing active methanogenesis under field
121 conditions, where organic matter, nutrients and organisms can be exchanged within the
122 whole soil profile, thereby promoting methanogenesis at the bottom of the active layer.

123 The multi-annual incubations provided for the first time a dataset enabling the calibration of a
124 carbon decomposition model for predicting long-term $CO_2$ and $CH_4$ formation from thawing
125 permafrost. Under oxic conditions, the model predicts an average degradation of 113 ± 58 g
126 $CO_2$-C $kg^{-1}$ of permafrost organic carbon until 2100 (Fig. 3a), when assuming microbial
127 activity during four months per year, which represents the short summer thaw period of
128 permafrost soils (see Methods). These model results are in the range of current estimates of
129 oxic long-term permafrost organic carbon decomposition[15, 25, 26]. Under anoxic conditions, the
130 $CO_2$ production accounts for 17 ± 9.3 g $CO_2$-C $kg^{-1}$ of initial permafrost carbon and $CH_4$
131 production releases 22 ± 13 g $CH_4$-C $kg^{-1}$ of permafrost carbon (Fig. 3a, Suppl. Table S5).
132 However, when comparing the GHG production under oxic and anoxic conditions based on
133 $CO_2$-C equivalents, i.e. by considering a GWP of 28 for $CH_4$ (weight corrected), the GHG
134 release under anoxic conditions is on average 2.4 ± 1.2 times higher than under oxic
135 conditions (Fig. 3b; H2; Suppl. Table S5). These observation-calibrated long-term estimates
136 of anoxic $CO_2$ and $CH_4$ production contradict recent studies reporting a minor importance of

137 methanogenesis and a lower GHG production after permafrost thaw under water-saturated,
138 anoxic conditions[3, 4, 7, 12].

139 The predicted formation of $CH_4$ over 90 years (until 2100) would relate to an annual
140 production of about 0.24 g $CH_4$-C $kgC^{-1}$ $yr^{-1}$. These rates are lower than maximum $CH_4$
141 production rates (1.2 g $CH_4$-C $kgC^{-1}$ $yr^{-1}$) reported from mainly short term incubation studies[12]
142 but our long-term estimates are likely more relevant for predicting GHG production from
143 thawing permafrost on climate relevant time scales. Decadal-scale (60 yr) *in situ* $CH_4$
144 production rates (0.50 g $CH_4$-C $kgC^{-1}$ $yr^{-1}$) from thawing permafrost surrounding arctic
145 thermokarst lakes[27], are close to our estimates even though our model considers $CH_4$
146 formation only during 4 months of summer thaw while unfrozen thermokarst lake sediments
147 produce $CH_4$ year round. However, *in situ* $CH_4$-fluxes from thawing permafrost in two boreal
148 peatlands (0.02-0.04 g $CH_4$-C $kgC^{-1}$ $yr^{-1}$)[24] are below the range of our long-term estimates
149 (0.09–0.46 g $CH_4$-C $kgC^{-1}$ $yr^{-1}$), which indicates a low decomposability of the woody and
150 *Sphagnum* peat in these peatlands[24] but might also be influenced by $CH_4$ oxidation during
151 $CH_4$ transport from the anoxic peat into the atmosphere[23].

152 Permafrost soils contain in their permanently frozen subsurface substantial amounts of
153 organic matter since its decomposition was prevented by freezing temperatures[9].
154 Furthermore, permafrost impedes water drainage, causing a widespread occurrence of
155 water-saturated soils and sediments in the northern permafrost region[11]. We can therefore
156 assume a high relevance of anaerobic permafrost carbon mineralization also at the pan-
157 Arctic scale. To contribute to this discussion, we combined, in a simplified assessment, the
158 results from our decomposition model with data from permafrost carbon profiles and thawing
159 depth simulations (see Suppl. Information). In this scenario, less than one third of thawing
160 permafrost organic carbon would thaw until 2100 under water-saturated conditions (Suppl.
161 Table S6) and the carbon release from thawing permafrost would be substantially higher
162 under non-saturated conditions (2.6 ± 3.2 Pg – 9.5 ± 7.0 Pg $CO_2$-C) than under saturated
163 conditions (0.4 ± 0.6 Pg – 1.4 ± 1.4 Pg $CO_2$-C and $CH_4$-C). But due to the equal share of $CO_2$

and $CH_4$ formation under water-saturated conditions, the GHG production from permafrost thawing at the bottom of water-saturated soils, if expressed as $CO_2$-C equivalents (2.4 ± 3.7 Pg – 8.9 ± 8.8 Pg $CO_2$-C equivalents, Suppl. Table S6), would almost equal those under non-saturated conditions at the pan-Arctic scale. The large uncertainty in these estimates reflect the simplicity of our calculation, which was intended to assess the importance of anoxic decomposition pathways for GHG production in permafrost regions and encourage further spatially explicit approaches. Methane production rates in organic permafrost soils, which store about 14% of organic carbon in permafrost landscapes[9], were generally found to be higher than in mineral soils[6, 12], even if this is not always the case[24]. Since we incubated only mineral soil samples, our spatial extrapolation on potential $CH_4$ production from thawing permafrost organic carbon is therefore likely conservative.

However, GHG production in thawing permafrost cannot be directly transcribed into GHG emissions to the atmosphere since a variable fraction of $CH_4$ produced in thawing permafrost will be oxidized by microorganisms to $CO_2$ when passing oxic soil or sediment layers[23, 28]. In this context, the vegetation composition plays a crucial role since many vascular wetland plants channel $CH_4$ from its production zone into the atmosphere thereby circumventing its oxidation[23]. However, even relatively low $CH_4$ fluxes may turn northern wetlands from a carbon sink into a GHG source (based on $CO_2$-C equivalents) when considering the higher GWP of $CH_4$ [29, 30].

Our results from laboratory incubations and numerical modelling, which for the first time enable a direct comparison of $CO_2$ and $CH_4$ formation in thawing permafrost on climate relevant time scales, contradict the current view of a stronger permafrost-carbon climate feedback from drained, oxic soils and provide the first data-informed projection of long-term $CH_4$ production from thawing permafrost. Sound predictions on the future pan-Arctic release of $CO_2$ and $CH_4$ from thawing permafrost need a better understanding on future wetland distribution and hydrology in the permafrost region as well as on *in situ* $CH_4$ production in

water saturated permafrost soils including organic soils, which will play a key role for $CH_4$ fluxes from permafrost landscapes.

**References:**


1. Schuur EAG, McGuire AD, Schädel C, Grosse G, Harden JW, Hayes DJ*, et al.* Climate change and the permafrost carbon feedback. *Nature* 2015, **520**(7546)**:** 171-179.

2. McGuire AD, Chapin III FS, Walsh JE, Wirth C. Integrated regional changes in arctic climate feedbacks: Implications for the global climate system. *Annual Review of Environment and Resources* 2006, **31**(1)**:** 61-91.

3. Lee H, Schuur EAG, Inglett KS, Lavoie M, Chanton JP. The rate of permafrost carbon release under aerobic and anaerobic conditions and its potential effects on climate. *Global Change Biology* 2012, **18**(2)**:** 515-527.

4. Treat CC, Wollheim WM, Varner RK, Grandy AS, Talbot J, Frolking S. Temperature and peat type control $CO_2$ and $CH_4$ production in Alaskan permafrost peats. *Global Change Biology* 2014, **20:** 2674-2686.

5. Waldrop MP, Wickland KP, White III R, Berhe AA, Harden JW, Romanovsky VE. Molecular investigations into a globally important carbon pool: permafrost-protected carbon in Alaskan soils. *Global Change Biology* 2010, **16**(9)**:** 2543-2554.

6. Roy Chowdhury T, Herndon EM, Phelps TJ, Elias DA, Gu B, Liang L*, et al.* Stoichiometry and temperature sensitivity of methanogenesis and $CO_2$ production from saturated polygonal tundra in Barrow, Alaska. *Global Change Biology* 2015, **21**(2)**:** 722-737.

7. Schädel C, Bader MKF, Schuur EAG, Biasi C, Bracho R, Capek P*, et al.* Potential carbon emissions dominated by carbon dioxide from thawed permafrost soils. *Nature Climate Change* 2016, **6:** 950-953.

8. Myhre G, Shindell D, Bréon F-M, Collins W, Fuglestvedt J, Huang J*, et al.* Anthropogenic and Natural Radiative Forcing. In: Stocker TF, Qin D, Plattner G-K, Tignor M, Allen SK, Boschung J*, et al.* (eds). *Climate Change 2013: The Physical Science Basis. Contribution of Working Group I to the Fifth Assessment Report of the Intergovernmental Panel on Climate Change*. Cambridge University Press: Cambridge, United Kingdom and New York, USA, 2013, pp 659-740.

9. Hugelius G, Strauss J, Zubrzycki S, Harden JW, Schuur EAG, Ping C-L*, et al.* Estimated stocks of circumpolar permafrost carbon with quantified uncertainty ranges and identified data gaps. *Biogeosciences* 2014, **11**(23)**:** 6573-6593.

10. Jorgenson MT, Harden J, Kanevskiy M, O'Donnell J, Wickland K, Ewing S*, et al.* Reorganization of vegetation, hydrology and soil carbon after permafrost degradation

across heterogeneous boreal landscapes. *Environmental Research Letters* 2013, **8**(3).

11. Bring A, Fedorova I, Dibike Y, Hinzman L, Mård J, Mernild SH*, et al.* Arctic terrestrial hydrology: A synthesis of processes, regional effects, and research challenges. *Journal of Geophysical Research: Biogeosciences* 2016, **121**(3)**:** 621-649.

12. Treat CC, Natali SM, Ernakovich J, Iversen CM, Lupascu M, McGuire AD*, et al.* A pan-Arctic synthesis of $CH_4$ and $CO_2$ production from anoxic soil incubations. *Global Change Biology* 2015, **21**(7)**:** 2787-2803.

13. Natali SM, Schuur EAG, Mauritz M, Schade JD, Celis G, Crummer KG*, et al.* Permafrost thaw and soil moisture driving $CO_2$ and $CH_4$ release from upland tundra. *Journal of Geophysical Research-Biogeosciences* 2015, **120**(3)**:** 525-537.

14. Johnston CE, Ewing SA, Harden JW, Varner RK, Wickland KP, Koch JC*, et al.* Effect of permafrost thaw on $CO_2$ and $CH_4$ exchange in a western Alaska peatland chronosequence. *Environmental Research Letters* 2014, **9**(10).

15. Knoblauch C, Beer C, Sosnin A, Wagner D, Pfeiffer E-M. Predicting long-term carbon mineralization and trace gas production from thawing permafrost of Northeast Siberia. *Global Change Biology* 2013, **19**(4)**:** 1160-1172.

16. Liebner S, Ganzert L, Kiss A, Yang SZ, Wagner D, Svenning MM. Shifts in methanogenic community composition and methane fluxes along the degradation of discontinuous permafrost. *Frontiers in Microbiology* 2015, **6:** 10.

17. Angel R, Claus P, Conrad R. Methanogenic archaea are globally ubiquitous in aerated soils and become active under wet anoxic conditions. *ISME J* 2012, **6**(4)**:** 847-862.

18. Ping CL, Jastrow JD, Jorgenson MT, Michaelson GJ, Shur YL. Permafrost soils and carbon cycling. *SOIL* 2015, **1**(1)**:** 147-171.

19. Voigt C, Lamprecht RE, Marushchak ME, Lind SE, Novakovskiy A, Aurela M*, et al.* Warming of subarctic tundra increases emissions of all three important greenhouse gases – carbon dioxide, methane, and nitrous oxide. *Global Change Biology* 2017, **23**(8)**:** 3121-3138.

20. Symons GE, Buswell AM. The methane fermentation of carbohydrates. *Journal of the American Chemical Society* 1933, **55**(5)**:** 2028-2036.

21. Nilsson M, Öquist M. Partitioning litter mass loss into carbon dioxide and methane in peatland ecosystems. In: Baird AJ, Belyea LR, Comas X, Reeve AS, Slater LD (eds). *Carbon Cycling in Northern Peatlands*, vol. 184. Amer Geophysical Union: Washington, 2009, pp 131-144.

22. Hodgkins SB, Tfaily MM, McCalley CK, Logan TA, Crill PM, Saleska SR*, et al.* Changes in peat chemistry associated with permafrost thaw increase greenhouse gas production. *Proceedings of the National Academy of Sciences* 2014, **111**(16)**:** 5819-5824.

23. Knoblauch C, Spott O, Evgrafova S, Kutzbach L, Pfeiffer E-M. Regulation of methane production, oxidation and emission by vascular plants and bryophytes in ponds of the northeast Siberian polygonal tundra. *Journal of Geophysical Research: Biogeosciences* 2015, **120:** 2525–2541.

24. Cooper MDA, Estop-Aragones C, Fisher JP, Thierry A, Garnett MH, Charman DJ*, et al.* Limited contribution of permafrost carbon to methane release from thawing peatlands. *Nature Climate Change* 2017, **7**(7)**:** 507-511.

25. Schädel C, Schuur EAG, Bracho R, Elberling B, Knoblauch C, Lee H*, et al.* Circumpolar assessment of permafrost C quality and its vulnerability over time using long-term incubation data. *Global Change Biology* 2014, **20**(2)**:** 641-652.

26. Elberling B, Michelsen A, Schädel C, Schuur EAG, Christiansen HH, Berg L*, et al.* Long-term $CO_2$ production following permafrost thaw. *Nature Climate Change* 2013, **3**(10)**:** 890-894.

27. Walter Anthony K, Daanen R, Anthony P, Schneider von Deimling T, Ping C-L, Chanton JP*, et al.* Methane emissions proportional to permafrost carbon thawed in Arctic lakes since the 1950s. *Nature Geoscience* 2016, **9:** 679-682.

28. Popp TJ, Chanton JP, Whiting GJ, Grant N. Evaluation of methane oxidation in the rhizosphere of a *Carex* dominated fen in north central Alberta, Canada. *Biogeochemistry* 2000, **51**(3)**:** 259-281.

29. Friborg T, Soegaard H, Christensen TR, Lloyd CR, Panikov NS. Siberian wetlands: Where a sink is a source. *Geophysical Research Letters* 2003, **30**(21)**:** 4.

30. Wille C, Kutzbach L, Sachs T, Wagner D, Pfeiffer E-M. Methane emission from Siberian arctic polygonal tundra: Eddy covariance measurements and modeling. *Global Change Biology* 2008, **14:** 1395–1408.

## Additional information

Supplementary information is available for this manuscript. Correspondence and requests for materials should be addressed to C.K.

## Acknowledgements

We gratefully acknowledge the financial support through the Cluster of Excellence “CliSAP” (EXC177), University Hamburg, funded through the German Research Foundation (DFG), the CarboPerm project funded by the German Ministry for Research and Education (03G0836A) to C.K. C.B. and E.M.P and the Helmholtz Gemeinschaft (HGF) by funding the Helmholtz Young Investigators Group of S.L. (VH-NG-919). Special thanks to G. Hugelius for valuable discussions, to D. Wagner and S. Zubrzycki for providing samples, to B. Schwinge for laboratory assistance, to Waldemar Schneider and Günter (Molo) Stoof for help during the field campaigns and the German and Russian colleagues from the Alfred Wegener Institute in Potsdam, the Lena Delta Reserve in Tiksi and the Tiksi Hydrobase for logistical support.

## Author contributions

C.K. and C.B designed the study. CK., E.M.P and M.N.G. did the field work. C.K. conducted the incubation experiment, C.B. calibrated the model and predicted site-level and pan-Arctic GHG production, S.L. quantified the methanogen abundance. C.K. and C.B wrote the manuscript with contribution of all co-authors.

## Competing financial interests

The authors declare no competing financial interests.

## Methods

**Soil sampling and sample description.** Permafrost samples were collected from two islands in the northeast Siberian Lena Delta situated in the zone of continuous, deep permafrost. The mean annual air temperature at the sampling sites is -12.5 °C and the permafrost temperature is -9 °C[31]. Samoylov Island (72.369 N, 126.475 E) is comprised of Holocene permafrost deposits and characterized by polygonal tundra with alternating water-saturated polygon centers and drier polygon rims. Soils in the wet polygon centers were classified as Typic Historthels and at the drier rims as Typic Aquiturbels[32]. The vegetation is composed of two strata, a moss / lichen layer and a grass / sedge layer. The dominant vascular plant is *Carex aquatilis*[32] which is most abundant in the moist polygon centers. The surface active layer thaws for about four months per year to a mean depth of 50 cm[31]. Kurungnakh Island (72.333 N, 126.283 E) is composed of late Pleistocene Ice complex deposits (Yedoma) and characterized by polygonal tundra and widespread thermokarst features[33]. Samples from Samoylov (n=9) were collected from 0.6 to 4.3 m depth ($^{14}$C age 0.18 – 2.5 ka). The samples from Kurungnakh were taken from the permafrost surface (0.7 m) to a depth of 23 m. Between 0.7 m and 2.5 m the carbon was of Holocene age ($^{14}$C age 2.3 to about 8.7 ka, n=4). Pleistocene samples from below were deposited during the last glacial maximum (Sartan, 3.1 - 11.7 m depth, $^{14}$C ages of about 14 to 29 ka, n=10) and the late Pleistocene optimum (Kargin, 16 - 23 m depth, $^{14}$C ages of about 34 to 42 ka, n=6). Organic carbon concentrations in the Samoylov samples ranged between 0.6 and 6.8% and in the Kurunkgnakh samples between 0.6 and 12.4% with highest concentrations in the Holocene and lowest concentrations in the Sartan deposits. All samples were collected in frozen state and stored frozen until processing in the laboratory. Further details on sampling and sample characteristics are given in ref 15 and Suppl. Table S1.

**Stable isotope labelling of *Carex aquatilis***. *Carex aquatilis* plants were labelled with $^{13}CO_2$ at a water inundated site on Samoylov in July 2008. Before labelling, all *C. aquatilis* leaves were clipped below the water table. Subsequently an area of 0.5 x 0.5 m was covered every

day between 11:00 and 15:00 with a transparent chamber (0.25 m high) to which 98 atom% $^{13}CO_2$ was added, to reach about twice ambient concentrations of $CO_2$. After three weeks, the fresh $^{13}C$-labelled leave biomass was clipped above the water table.

**Incubation experiments.** The setup of the initial incubation experiment has been described in detail in ref 15. Briefly, samples were thawed in a refrigerator at about 2 °C. Six aliquots of about 20 g fresh weight were placed in sterile 120 ml incubation flasks that were closed with sterile butyl rubber stoppers. Samples for anoxic incubations were processed first and handled under a constant flow of sterilized molecular nitrogen to minimize oxygen exposure. The anoxic incubations (three replicates) were amended with 5 ml of anoxic, sterile water and the headspace was repeatedly exchanged with pure sterilized nitrogen to establish anoxic conditions. No water was added to the other three replicates, which were incubated under oxic conditions. $CO_2$ and $CH_4$ concentrations in the headspace of all replicates were measured with a gas chromatograph (7890, Agilent Technologies, USA)[15]. The total amount of $CO_2$ and $CH_4$ was calculated from the partial pressure of the gases, the temperature, the head space volume, the amount of water and the water solubility of $CH_4$ (ref 34) and $CO_2$ by also considering carbonate and bicarbonate concentrations at the given pH (ref 35), which ranged between 4.0 and 8.1 (see Suppl. Table S1). A timeline of the incubation experiment is given in Suppl. Fig. S1. All $CO_2$ and $CH_4$ production data are normalized to gram permafrost organic carbon if not stated otherwise. Samples were incubated at 4 °C. Since $CH_4$ production only started after a lag-phase of few weeks up to several years (mean 635 ± 620 d, n=60, Suppl. Table S1) aerobic and anaerobic samples were pre-incubated with three replicates both under oxic and anoxic conditions for four years until most of the anoxically incubated samples established a stable methane producing community (pre-incubation). Subsequently, 12 representative samples that passed maximum $CH_4$ production rates were selected for the main experiment (Suppl. Table S1). Preference was given to surface samples where permafrost thaw is expected to be most pronounced and to samples with still three oxic and anoxic replicates available. At the onset of the main experiment, the organic carbon that was respired during the pre-incubation phase was backfilled with $^{13}C$-labelled

399 organic matter from *Carex aquatilis* ($\delta^{13}C$ = 774 ‰ VPDB). The addition of structural carbon
400 from *C. aquatilis*, the most abundant vascular plant at the sampling sites, was aimed to
401 simulate the input of fresh organic matter from the recent vegetation into the thawed
402 permafrost. After the addition of *Carex* plant material to the 12 samples selected for the main
403 experiment the samples were incubated under the same conditions as before for another
404 three years.

405 The remaining 17 samples were continuously incubated at 4°C for another three years
406 (Suppl. Fig. S1). At the end of the incubation time of these samples (7 years) $CH_4$ production
407 was detectable in all except of four samples (Suppl. Table S1). To test if the lack of $CH_4$
408 production was due to the absence of a methanogen community, these samples were
409 inoculated with 1 ml of a permafrost sample containing an active methanogen community
410 (Kurungnakh, 21.0 – 21.7 m depth, $^{14}C$-age 40.0 ka). After inoculation, the samples were
411 incubated for another 0.6 years at 4°C and $CH_4$ and $CO_2$ concentrations were measured
412 repeatedly. Before inoculation and at the end of the 0.6 years incubation, subsamples were
413 taken from these four samples and the inoculum to quantify the mcrA-gene as marker for
414 methanogenic archaea (Suppl. Table S2).

415 **Partitioning of $CO_2$ and $CH_4$ production into permafrost organic carbon and *Carex***
416 **organic carbon.** A simple two endmember model[36] was applied to partition the total amount
417 of $CO_2$ and $CH_4$ produced in the main experiment into $CO_2$ and $CH_4$ originating from
418 permafrost organic carbon and $CO_2$ and $CH_4$ originating from *Carex* organic carbon. The
419 fraction of $CO_2$ or $CH_4$ originating from permafrost organic carbon was calculated according
420 to equation [1]:

421 [1] $f_{Poc}=(\delta^{13}C_{CO2,\ CH4} - \delta^{13}C_{Car}) / (\delta^{13}C_{Poc} - \delta^{13}C_{Car})$

422 With $f_{Poc}$ = fraction of $CO_2$ or $CH_4$ from permafrost organic carbon, $\delta^{13}C_{CO2,\ CH4}$ = the $\delta^{13}C$-
423 value of the released gas ($CO_2$ or $CH_4$), $\delta^{13}C_{Car}$ = the $\delta^{13}C$-value of the added *Carex* plant
424 material (774 ‰ VPDB), and $\delta^{13}C_{Poc}$ = the $\delta^{13}C$-value of the $CO_2$ or $CH_4$ at the end of the

pre-incubation phase, which only originated from permafrost organic carbon. The fraction of $CO_2$ or $CH_4$ originating from *Carex* organic matter was calculated according to equation [2]:

[2] $f_{Car} = 1 - f_{Poc}$

with $f_{Car}$ = fraction of produced $CO_2$ or $CH_4$ from *Carex* organic matter.

The partitioning of the produced $CO_2$ and $CH_4$ during the main experiment was done for each measurement (aerobic incubations: n = 21, anaerobic incubations: n = 16) for each of the replicates.

**Stable carbon isotope analysis.** The $\delta^{13}C$-values of $CO_2$ and $CH_4$ were determined with an isotope ratio mass spectrometer (ThermoQuest Finnigan, Delta Plus, Germany) equipped with a GC (Agilent, 6890, USA) and a GC/C III combustion unit (ThermoQuest Finnigan, Germany). The external standards IAEA NGS3 (-73.3 ‰ VPDB), LSVEC (-46.6 ‰ VPDB), and B7 (-3.0 ‰ VPDB) were used for unlabeled samples. $CO_2$ and $CH_4$ from the main experiment were measured against the IAEA standards 303A (93.3 ‰ VPDB) and 303B (466 ‰ VPDB) to account for the higher $\delta^{13}C$-values resulting from the degradation of the $^{13}C$-labelled organic matter of *C. aquatilis*.

**Organic matter dynamic decomposition model and extrapolation into future.** The cumulative $CO_2$ and $CH_4$ production from thawed permafrost organic carbon during the main experiment (three years incubation data after four years of pre-incubation) were used to calibrate an organic carbon decomposition model and simulate GHG formation from the thawed permafrost samples until 2100. The model follows the principles of the Introductory Carbon Balance Model—ICBM[15, 37]. A first-order kinetics equation represents the change of organic carbon content in time. This equation is applied to two carbon pools with high and low rate constants, respectively[38]. A fraction of the degrading material from the fast decomposable pool (labile pool) flows into the slower decomposable pool (stable pool), which represents stabilization of organic carbon due to a variety of soil processes. The remaining part leaves the system as the trace gases $CO_2$ or $CH_4$. The degradation of the

451 more stable pool is assumed to fully contribute to the trace gas flux. The initial condition of
452 total organic carbon content is prescribed by observations. The initial fraction of the labile
453 pool is treated as a parameter and the initial fraction of the stable organic carbon pool is then
454 calculated as the difference to the total organic carbon content. Using a nonlinear least-
455 squares approach with a trust-region-reflective algorithm in MATLAB R2015a (MathWorks
456 Inc., USA), the following four model parameters have been optimized: two turnover times
457 (labile and stabile pool), initial labile carbon pool fraction, and the stabilization coefficient.
458 The model was calibrated against the cumulative GHG production from each sample and
459 replicate. Then, the calibrated model was run forward for 90 years for each sample and
460 replicate. In doing so, microbial decomposition processes were assumed to be constantly
461 active during four summer months at the temperature of incubation (4 °C) following recent
462 observations at the sampling sites[31]. The model results for aerobic $CO_2$ production and
463 anaerobic $CO_2$ and $CH_4$ production were reported relative to the initial organic carbon content
464 of the respective permafrost samples (Fig. 3a). The results for $CH_4$ production were also
465 multiplied by the GWP of $CH_4$ (weight corrected) to compare aerobic and anaerobic GHG
466 production based on $CO_2$-C equivalents (Fig. 3b). Data on projected organic carbon
467 degradation were tested for normal distribution by using the Kolmogorov-Smirnov test with
468 Lilliefors correction. Calibrating the carbon decomposition model with the incubation data of
469 only the first year of the main experiment (after 4 years of pre-incubation) produced similar
470 results than if using the whole dataset of three years (Suppl. Fig. S2).

471 **Quantification of the methanogen community.** Total genomic DNA was extracted in
472 duplicates using the PowerSoil DNA extraction kit (MO BIO laboratories, USA) according to
473 the manufacturer's protocol with the modification that samples were homogenized through
474 grinding in liquid nitrogen prior to the extraction. DNA was extracted only from replicates of
475 those four samples showing no $CH_4$ production after 7 years, from the same samples 0.6
476 years after being inoculated with active methanogens and from the samples used as
477 inoculum for the inactive samples (Suppl. Table S2). Quality and quantity of the DNA was
478 assessed through gel electrophoresis and photometry (NanoPhotometer, Implen, Germany).

The enumeration of methanogenic gene copies was realized through quantitative PCR (qPCR) as described elsewhere[16] targeting the *mcrA*- gene (methanogens). Briefly, SybrGreen qPCR assays were run on a CFX96TM cycler (Bio-Rad Laboratories, USA). Each qPCR run included *mcrA*-gene copies of *M. barkeri* as calibration standards and blanks and was performed in triplicates. Ahead of the final qPCR run, several sample dilutions were tested for potential inhibition. We used a final primer concentration of 0.4 µM and 10 µl 2x SensiFAST SYBR Mix (KAPA Biosystems, USA) in 20 µl reactions. The specificity of each run was verified through melt-curve analysis and gel electrophoresis. The *mcrA*-gene was amplified with the primers mlas and mcrA-rev[39] with annealing at 55 °C for 20 s.

**Data availability.** The data that support the findings of this study and that are not presented within the article and its supplementary information file are available from C.K. on reasonable request.

## Methods only References


31. Boike J, Kattenstroth B, Abramova K, Bornemann N, Chetverova A, Fedorova I*, et al.* Baseline characteristics of climate, permafrost and land cover from a new permafrost observatory in the Lena River Delta, Siberia (1998-2011). *Biogeosciences* 2013, **10**(3)**:** 2105-2128.

32. Kutzbach L, Wagner D, Pfeiffer E-M. Effect of microrelief and vegetation on methane emission from wet polygonal tundra, Lena Delta, Northern Siberia. *Biogeochemistry* 2004, **69:** 341-362.

33. Morgenstern A, Ulrich M, Günther F, Roessler S, Fedorova IV, Rudaya NA*, et al.* Evolution of thermokarst in East Siberian ice-rich permafrost: A case study. *Geomorphology* 2013, **201:** 363-379.

34. Yamamoto S, Alcauskas JB, Crozier TE. Solubility of methane in distilled water and seawater. *Journal of Chemical and Engineering Data* 1976, **21**(1)**:** 78-80.

35. Millero F, Huang F, Graham T, Pierrot D. The dissociation of carbonic acid in NaCl solutions as a function of concentration and temperature. *Geochimica et Cosmochimica Acta* 2007, **71**(1)**:** 46-55.

36. Amundson R, Baisden WT. Stable isotope tracers and mathematical models in soil organic matter studies. In: Sala OE, Jackson RB, Mooney HA, Howarth RB (eds). *Methods in Ecosystem Science*. Springer New York, 2000, pp 117-137.

37. Andrén O, Kätterer T. ICBM: The introductory carbon balance model for exploration of soil carbon balances. *Ecological Applications* 1997, **7**(4)**:** 1226-1236.

38. Meentemeyer V. Macroclimate and lignin control of litter decomposition rates. *Ecology* 1978, **59**(3)**:** 465-472.

39. Steinberg LM, Regan JM. mcrA-targeted real-time quantitative PCR method to examine methanogen communities. *Appl Environ Microbiol* 2009, **75**(13)**:** 4435-4442.

## Figure Captions

Figure 1: Methane production in a permafrost sample from Kurungnakh Island (10.9-11.7 m depth) that did not show $CH_4$ production during 2,500 days of incubation and was then inoculated with a sample from the same sampling site (21.0 – 21.7 m depth) containing active methanogens. Data are means of two replicates, ± SD. The arrow gives the time of inoculation.

Figure 2: Calibration of a two-pool carbon decomposition model with the obtained observational data. **(a)** Oxic $CO_2$ production and **(b)** anoxic $CO_2$ and $CH_4$ production in a permafrost sample from Samoylov Island (2.8-3.1 m depth, mean of n=3, ± SD). The lines represent the mean values of the model results from three replicates. The insert in **(b)** shows the ratio of $CO_2$:$CH_4$ produced during the main experiment for all 12 samples. The box gives the 75% and 25% percentile, the whiskers the 99% and 1% percentile. The horizontal line stands for the median value and the cross shows the arithmetic mean. All values are expressed relative to permafrost organic carbon.

Figure 3: Prediction of $CO_2$ and $CH_4$ production from thawing permafrost organic carbon until 2100. **(a)** $CO_2$ and $CH_4$ production relative to the initial organic carbon content of permafrost. **(b)** Comparison of oxic and anoxic GHG production relative to the initial organic carbon content of permafrost after conversion of $CH_4$ production to $CO_2$-C equivalents ($CO_2$-Ceq.) assuming a GWP of 28 for $CH_4$. The boxes in both panels give the 75% and 25% percentile, the whiskers the approximately 99% and 1% percentile. The horizontal lines stand for the median values and the crosses show the arithmetic means of 12 samples.

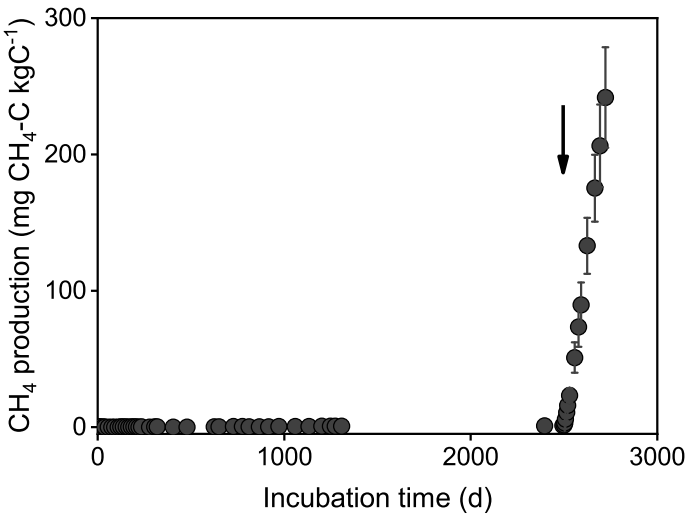


Fig. 1, Knoblauch et al. 2018

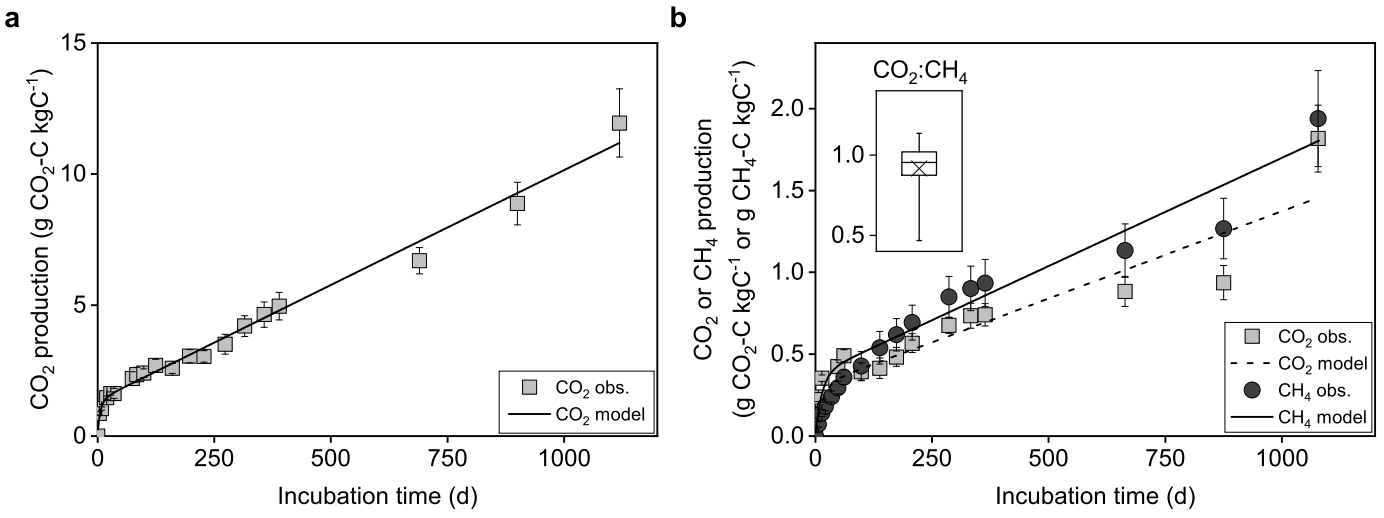


Fig. 2, Knoblauch et al. 2018

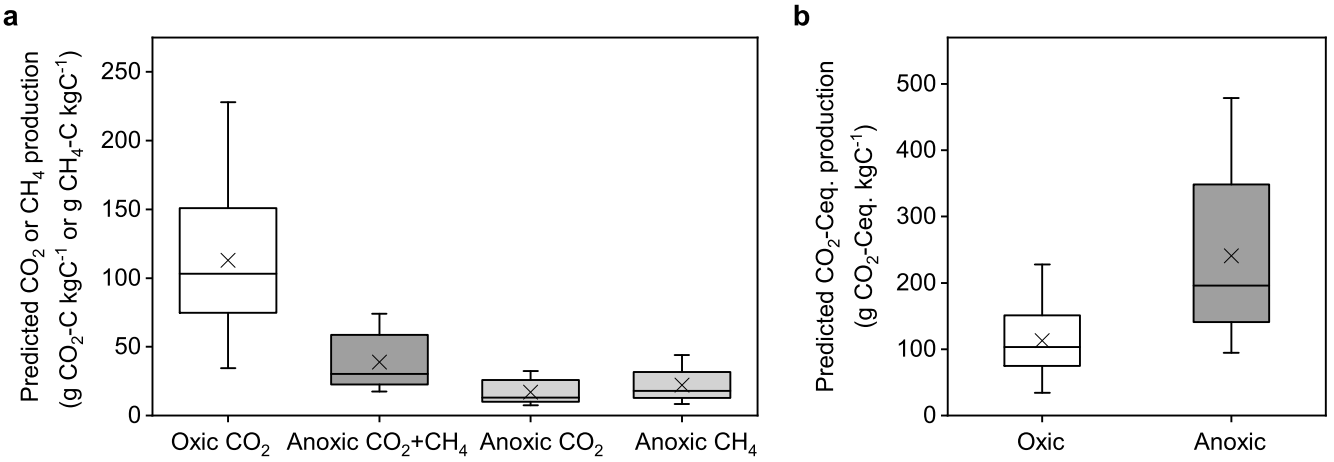


Fig. 3, Knoblauch et al., 2018

**Methane production as key to the greenhouse gas budget of thawing permafrost**

Christian Knoblauch[1, 2*], Christian Beer[3, 4], Susanne Liebner[5], Mikhail N. Grigoriev[6], Eva-Maria Pfeiffer[1, 2]

[1]Institute of Soil Science, Universität Hamburg, Hamburg, Germany
[2]Center for Earth System Research and Sustainability, Universität Hamburg, Hamburg Germany
[3]Department of Environmental Science and Analytical Chemistry, Stockholm University, Stockholm, Sweden
[4]Bolin Centre for Climate Research, Stockholm University, Stockholm, Sweden
[5]GFZ German Research Centre for Geosciences, Section Geomicrobiology, Potsdam, Germany
[6]Siberian Branch, Russian Academy of Sciences, Mel'nikov Permafrost Institute, Yakutsk, Russia

## Additional Results:

### Effect of *Carex* amendment on permafrost organic carbon decomposition

To account for the effect of the added *Carex aquatilis* organic matter on $CO_2$ and $CH_4$ production from permafrost organic carbon during the main experiment (priming effect), we compared the rates of $CO_2$ and $CH_4$ production from permafrost organic matter at the end of the pre-incubation phase (without *Carex* addition) with those during the main experiment (with *Carex* addition). Differences were expected preferentially at the beginning of the main experiment, when labile organic matter from the *Carex* plant litter is available. We observed only an increase of $CO_2$ and $CH_4$ production rates (positive priming) during a relatively short period of three to six weeks at the beginning of the main experiment. Supplementary Table S3 shows the duration of the period with $CO_2$ and $CH_4$ production rates above those at the end of the pre-incubation phase.

Furthermore, the contribution of additional $CO_2$ and $CH_4$ production due to priming of permafrost organic matter decomposition was calculated relative to the total amount of $CO_2$ or $CH_4$ production during the main experiment using equation S1:

[S1] $$P_p = \frac{P_i - R_{pi} * D}{P_{me}} * 100$$

with $P_p$ = additional production of $CO_2$ or $CH_4$ due to priming (in % of total production during the main experiment), $P_i$ = total amount of $CO_2$ or $CH_4$ produced during the initial phase of the main experiment with elevated decomposition rates from permafrost organic matter (see Suppl. Table S3), $R_{pi}$ = rate of $CO_2$ or $CH_4$ production at the end of the pre-incubation phase, D = duration of elevated $CO_2$ and $CH_4$ production rates at the beginning of the pre-incubation

phase (see Suppl. Table S3), $P_{me}$ = total amount of $CO_2$ or $CH_4$ produced during the main experiment.

The priming effect, i.e. the acceleration of permafrost organic matter decomposition due to the addition of labile *Carex aquatilis* litter, caused only a relatively small increase of total permafrost organic carbon decomposition over the whole main experiment (Suppl. Table S3). The highest effect was found for anaerobic $CO_2$ production (average ± SD: 13.3 ± 10.4 % of total $CO_2$ production) and the lowest effect for anaerobic $CH_4$ production (average ± SD: 5.8 ± 5.0 % of total $CH_4$ production).

**Assessment of GHG production from permafrost thawing at pan-Arctic scale**

In a first step we estimated the amount of volume of currently frozen soil sediments that will thaw until 2100 based on future projections of active-layer thickness (ALT) deepening as reported in figure 2 of ref 1 for two Representative Concentration Pathways (RCP4.5 and RCP8.5). For this we subtracted the area below each RCP cumulative ALT distribution curve for 2099 from the area below the simulation of the current cumulative ALT distribution curve in that figure. For this integration we defined 7 soil layers such that the cumulative distribution curve can be assumed to be linear (0.3, 0.5, 1, 1.5, 2, 2.5, 3 m depth) and applied the simple rectangle method of integration.

In a second step, we estimated the total content of thawing carbon by multiplying this volume of thawing permafrost soil by the mean carbon density reported for the above defined soil layers using data presented in figure 2 of ref 2. This calculation was done separately for Histels, and gleyed and non-gleyed parts of Turbels and Orthels, respectively. These statistics include all soil horizons including the O horizons. Histels and gleyed parts of Turbels and Orthels are assumed to be anoxic while all other parts of the Turbel and Orthel profiles are assumed to be oxic. In order to account for physical limitations of soil profiles in the field, e.g. depth to bedrock, these profile statistics per depth, in a third step, were further weighted according to vertically stratified results for Histels, Turbels and Orthels at the pan-Arctic scale[3]. Then, these estimates were scaled by the area of Turbels, Orthels and Histels from ref 3 for calculating the amount of oxic versus anoxic permafrost organic carbon thawing until 2100 in a fourth step. Permafrost thaw is a gradual and not an instantaneous process and we assume a linear thawing in time. Therefore, the increasingly available organic carbon under oxic and anoxic condition (Suppl. Table S6) was multiplied with our model results of the oxic and anoxic fraction of organic carbon decomposing into $CO_2$ and $CH_4$ until 2100 (Fig. 3a) and divided by two, thereby assuming a triangle below the time-evolution curve of ALT.

For estimating uncertainties of this GHG production at the pan-Arctic scale, a normal distribution of all oxic and anoxic organic carbon concentration profiles has been resampled (N=10,000) around the mean values reported in ref 2. For simplicity, we assumed a standard deviation similar to the mean value which is true for most of the soils and depths[2]. These distributions have been multiplied by all seven land surface model projections of permafrost thaw (see above) and all organic carbon degradation model results from the 12 samples times 3 replicates. Then, the mean and standard deviation of the resulting distributions of thawing organic carbon stocks and GHG productions were reported in Suppl. Table S6 and the text.

Depending on the future atmospheric GHG concentration pathways (RCP4.5 or RCP8.5), we estimate, with high uncertainty, 67 ± 70 Pg – 243 ± 127 Pg of current permafrost organic carbon to thaw and become available for microbial degradation (Suppl. Table S6). These numbers are lower than recently reported results[2], most probably since we used updated thaw projections[1]. In this scenario, less than one third the amount of organic carbon will thaw under water-saturated than under non-saturated conditions (Suppl. Table S6) and the GHG production in terms of carbon will be substantially higher in non-saturated soils (2.6 ± 3.2 Pg – 9.5 ± 7.0 Pg organic carbon into $CO_2$) than in saturated soils (0.4 ± 0.6 Pg – 1.4 ± 1.4 Pg organic carbon into $CO_2$ and $CH_4$). These figures only account for additional organic carbon mineralization from thawing permafrost, and exclude the surface active layer which thaws every summer, receives fresh organic matter from the surface vegetation and generally exhibits higher carbon decomposition rates than deeper permafrost layers[4, 5]. Hence, our estimates of permafrost carbon release are substantially lower than the range recently reported from spatially explicit approaches (21-174 Pg carbon) considering the whole soil column including the current active layer[1, 6]. Due to the equal contribution of $CO_2$ and $CH_4$ production to total GHG formation under oxic conditions and due to the higher GWP of $CH_4$, water-saturated soils are predicted to contribute equally to the overall GHG production from thawing permafrost if expressed as $CO_2$-C equivalents at a pan-Arctic scale (2.4 ± 3.7 Pg – 8.9 ± 8.8 Pg $CO_2$-C equivalents, Suppl. Table S6).

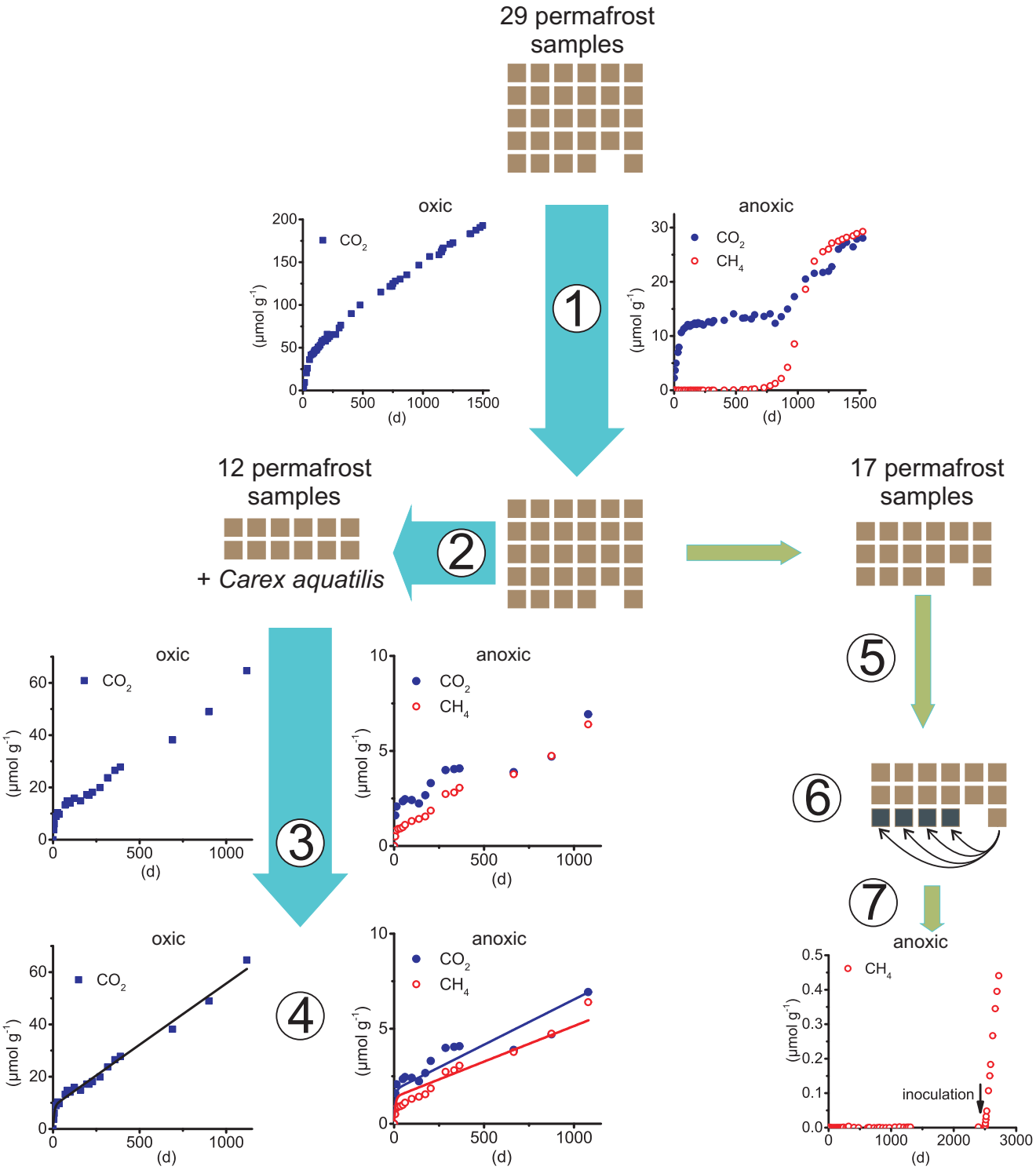


**Supplementary Figure S1:** Timeline of the incubation experiment. **1**: Pre-incubation of 29 permafrost samples for four years under oxic and anoxic conditions at 4 °C until constant $CO_2$ and $CH_4$ production rates have been established in most of the anoxic samples. **2**: Selection of 12 samples for the main experiment that passed maximum $CH_4$ production rates and refilling of the mineralized organic carbon with $^{13}C$-labelled organic carbon from *Carex aquatilis*. **3**: Quantification of $CO_2$ and $CH_4$ production from permafrost organic carbon under oxic and anoxic conditions for three years. **4**: Calibration of an organic carbon decomposition model with the cumulative $CO_2$ and $CH_4$ production from permafrost organic carbon. **5**: Incubation of the remaining 17 samples at 4 °C for 3 years. **6**: Inoculation of the 4 samples that showed no $CH_4$ production after 7 years of anaerobic incubation (black squares) with material from an active $CH_4$ producing permafrost sample. **7**: measurement of $CH_4$ production in inoculated samples for another 0.6 years. The small figures at steps 1 to 4 represent results from oxic (left panels, squares) and anoxic incubations (right panels, circles) of a sample from 4.1-4.3 m depth from Kurungnakh Island. The figure at step 7 shows results of a sample from 6.1-6.5 m depth from Kurungnakh Island (see Supplementary Table S1).

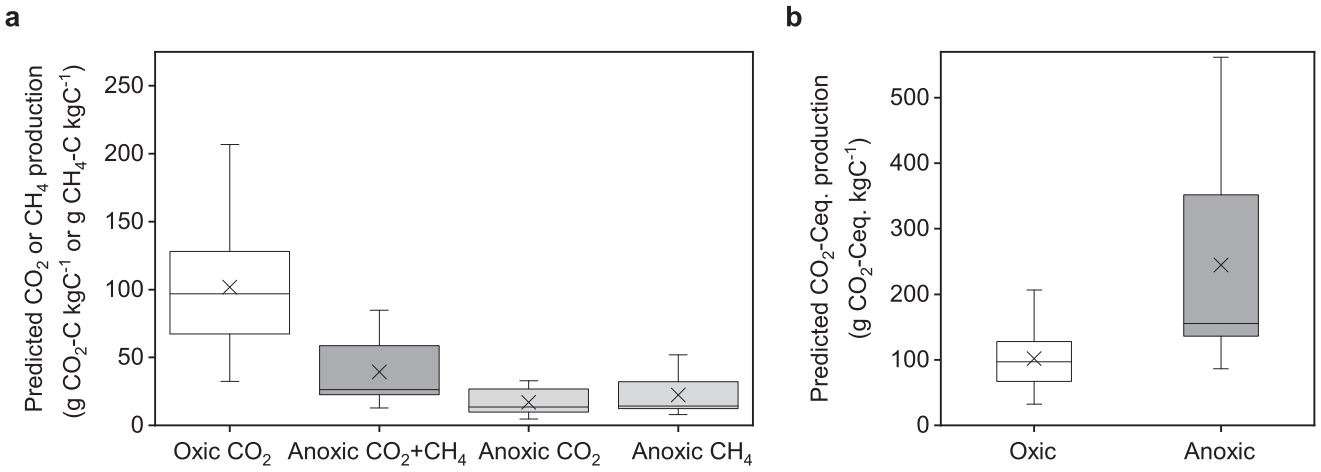


**Supplementary Figure S2:** Prediction of $CO_2$ and $CH_4$ production from thawing permafrost organic carbon until 2100 using only incubation data from the first year of the main experiment (after four years of pre-incubation). **(a)** $CO_2$ and $CH_4$ production relative to the initial organic carbon content of permafrost. **(b)** Comparison of oxic and anoxic GHG production relative to the initial organic carbon content of permafrost after conversion of $CH_4$ production to $CO_2$-C equivalents ($CO_2$-Ceq.) assuming a GWP of 28 for $CH_4$. The boxes in both panels give the 75% and 25% percentile, the whiskers the approximately 99% and 1% percentile. The horizontal lines stand for the median values and the crosses show the arithmetic means of 12 samples.

**Supplementary Table S1**: Sample characteristics of the incubated permafrost samples and gas production during the pre-incubation phase. Data on permafrost organic carbon ($C_{org}$), total nitrogen (N), C/N and pH were taken from ref 7. Samples in bold were selected for the main experiment. Values on gas production and lag-phase are means of generally three replicates with one standard deviation. GHG production is expressed relative to initial organic carbon content in permafrost samples. The surface soils at both sampling locations were classified as Turbic Cryosols[8].

| | | | | | | gas production until the end of pre-incubation | | | | | |
|---|---|---|---|---|---|---|---|---|---|---|---|
| Sampling site | Depth (m) | $C_{org}$ (%) | N (%) | C/N | pH | $CO_2$ oxic g $CO_2$-C kgC$^{-1}$ | $CO_2$ anoxic g $CO_2$-C kgC$^{-1}$ | $CH_4$ anoxic g $CH_4$-C kgC$^{-1}$ | ‡lag-phase (d) | max. $CH_4$ production g $CH_4$-C kgC$^{-1}$ yr$^{-1}$ | time until max. $CH_4$ production (d) |
| Samoylov | | | | | | | | | | | |
| | **0.6-0.8** | **0.60** | **0.04** | **16** | **6.2** | **58.6 ± 8.9** | **17.5 ± 4.7** | **10.7 ± 5.8** | **210 ± 58** | **4.9 ± 2.3** | **910 ± 237** |
| | **0.8-1.0** | **1.4** | **0.06** | **22** | **6.1** | **44.3 ± 0.9** | **12.2 ± 1.4** | **4.7 ± 0.7** | **173 ± 33** | **2.5 ± 0.4** | **1379 ± 0** |
| | **1.4-1.6** | **4.6** | **0.18** | **26** | **6.0** | **50.1 ± 4.5** | **12.3 ± 3.4** | **5.3 ± 1.6** | **53 ± 23** | **2.5 ± 0.1** | **635 ± 413** |
| | **1.9-2.1** | **4.4** | **0.20** | **22** | **5.8** | **44.7 ± 2.2** | **10.9 ± 1.1** | **6.6 ± 1.6** | **84 ± 3** | **4.5 ± 0.5** | **497 ± 54** |
| | 2.1-2.3 | 6.8 | 0.30 | 23 | 6.0 | 25.9 ± 2.5 | 5.3 ± 0.3 | 3.4 ± 0.3 | 91 ± 17 | 3.4 ± 0.5 | 447 ± 98 |
| | **2.8-3.1** | **4.8** | **0.20** | **24** | **6.4** | **35.9 ± 1.4** | **7.6 ± 0.5** | **5.1 ± 0.2** | **181 ± 3** | **3.4 ± 0.4** | **528 ± 54** |
| | **3.2-3.4** | **4.0** | **0.21** | **19** | **6.4** | **53.6 ± 8.7** | **9.6 ± 0.5** | **6.0 ± 0.8** | **197 ± 5** | **9.5 ± 2.8** | **678 ± 72** |
| | 3.7-3.9 | 3.2 | 0.21 | 15 | 6.6 | 46.4 ± 4.5 | 7.0 ± 1.2 | 2.3 ± 1.9 | 506 ± 77 | 3.4 ± 1.8 | 1468 ± 829 |
| | 4.1-4.3 | 1.9 | 0.13 | 15 | 6.7 | 25.8 ± 0.3 | 4.7 ± 0.2 | 2.4 ± 0.4 | 709 ± 242 | 3.9 ± 1.0 | 976 ± 274 |
| Kurungnakh | | | | | | | | | | | |
| | **0.7-0.8** | **3.9** | **0.20** | **19** | **4.0** | **25.8 ± 0.2** | **8.6 ± 0.5** | **1.3 ± 0.2** | **789 ± 44** | **1.2 ± 0.1** | **1248 ± 199** |
| | **0.9-1.1** | **12.4** | **0.78** | **16** | **4.8** | **31.8 ± 3.2** | **6.6 ± 1.0** | **2.4 ± 1.5** | **334 ± 52** | **3.2 ±0.5** | **1375 ± 143** |
| | **1.2-1.3** | **7.3** | **0.48** | **15** | **4.3** | **27.5 ± 3.1** | **6.6 ± 0.6** | **1.9 ± 0.3** | **439 ± 1** | **3.3 ± 0.5** | **1477 ± 0** |
| | 2.0-2.5 | 9.3 | 0.44 | 21 | 4.5 | 34.7 ± 5.4 | 4.0 ± 0.3 | ΨΨn.p. | 2182 ± 75 | 5.5 ± 0.5 | 3087 ± 0 |
| | 3.1-3.4 | 1.5 | 0.13 | 11 | 7.6 | 107.9 ± 6.7 | 15.0 ± 2.2 | 0.3 ± 0.4 | ¥935 | €0.8 | 1134 |
| | ***3.1-3.3** | **3.6** | **0.27** | **13** | **7.2** | **62.3 ± 8.0** | **17.1 ± 0.5** | **4.6 ± 4.0** | **1080 ± 737** | **7.7 ± 2.4** | **1333 ± 84** |
| | ***3.6-3.8** | **3.8** | **0.29** | **13** | **6.9** | **38.1 ± 1.5** | **5.7 ± 0.4** | **2.1 ± 0.5** | **820 ± 124** | **4.2 ± 0.9** | **1448 ± 48** |
| | 3.85 – 3.87 | 2.5 | 0.22 | 12 | 7.9 | 82.6 ± 3.7 | 15.2 ± 2.8 | ΨΨn.p. | > 2500 | #in | - |
| | ***4.1-4.3** | **4.9** | **0.35** | **14** | **7.2** | **46.6 ± 0.4** | **7.0 ± 0.4** | **6.8 ± 0.3** | **416 ± 83** | **11.4 ± 2.6** | **1019 ± 327** |
| | *4.6-4.8 | 6.0 | 0.48 | 12 | 7.1 | 50.9 ± 1.7 | 5.1 ± 1.2 | 6.3 ± 1.2 | 411 ± 84 | 8.0 ± 1.8 | 946 ± 330 |
| | 5.0-5.2 | 2.0 | 0.18 | 11 | 8.1 | 118.4 ± 3.7 | 18.0 ± 0.3 | ΨΨn.p. | 2286 ± 228 | 1.1 ± 0.8 | 2804 ± 105 |
| | 6.1-6.5 | 1.5 | 0.14 | 11 | 7.4 | 35.6 ± 1.6 | 8.5 ± 0.4 | ΨΨn.p. | > 2500 | #in | - |
| | 9.0-9.6 | 1.7 | 0.14 | 13 | 7.6 | 33.3 ± 0.3 | 8.8 ± 0.1 | ΨΨn.p. | > 2500 | #in | - |
| | 10.9-11.7 | 3.6 | 0.32 | 12 | 7.2 | 25.1 ± 1.1 | 6.6 ± 3.2 | ΨΨn.p. | > 2500 | #in | - |
| | 15.8-16.2 | 9.6 | 0.68 | 14 | 7.1 | 50.0 ± 2.0 | 9.4 ± 6.0 | 0.1 ± 0.1 | 877 ± 572 | €1.4 | 2729 |
| | 17.3-17.9 | 2.1 | 0.17 | 12 | 7.3 | 85.9 ± 7.3 | 12.9 ± 3.0 | 0.03 ± 0.03 | ¥1082 | §m.p.n.r | - |
| | *19.1-19.2 | 4.8 | 0.38 | 12 | 6.4 | 72.7 ± 2.4 | 5.0 ± 1.0 | ΨΨn.p. | £2315 | §m.p.n.r | - |
| | *19.9-20.0 | 4.8 | 0.36 | 13 | 7.2 | 109.9 ± 7.0 | 13.5 ± 1.7 | 1.9 ± 1.2 | 489 ± 8 | 1.6 ± 0.4 | 1988 |
| | 21.0-21.7 | 5.8 | 0.42 | 14 | 6.5 | 75.3 ± 0.6 | 16.7 ± 0.1 | 0.11 ± 0.02 | 950 ± 41 | 1.8 ± 0.1 | 2395 |
| | 22.3-22.5 | 0.58 | 0.04 | 16 | 6.8 | 49.1 ± 4.3 | 10.4 ± 0.7 | ΨΨn.p. | ¥1498 | €0.7 | 2501 |

‡lag-phase = time until 0.05 µmol $CH_4$ g$^{-1}$ was formed and $CH_4$ concentration continued increasing

ΨΨn.p. = no $CH_4$ production during the pre-incubation phase

*Samples taken from an outcrop, all other samples were collected from two cores drilled vertically into the permafrost, see ref. 7.

#in = inoculated after 2500 days with samples containing active methanogens (see Table S2)

€only one replicate reached maximum $CH_4$-production rates

¥only one replicate out of two showed $CH_4$ production

£only one replicate out of three showed $CH_4$ production

§ m.p.n.r. = maximum $CH_4$-production rates not reached in any of the replicates

**Supplementary Table S2:** Abundance of the *mcrA*-gene as marker for the abundance of methanogenic archaea in four samples without methanogenesis after seven years of anaerobic incubation, and $CH_4$ production rates after the inoculation of these samples with an active $CH_4$ producing sample (inoculum). Values are expressed relative to g dry weight permafrost soil.

| Sample | *mcrA*-gene abundance after 7 years ($10^5$ copies $g^{-1}$) | *mcrA*-gene abundance 0.6 years after inoculation ($10^5$ copies $g^{-1}$) | $CH_4$ production 0.6 years after inoculation (nmol $g^{-1}$ $d^{-1}$) |
|---|---|---|---|
| 21.0 - 21.7 m (inoculum) | 8.6 ± 3.8 | ¥n.d. | ¥n.d. |
| 3.85 - 3.87 m | *b.d.l. | 2.1 ± 0.6 | no production |
| 6.1 - 6.5 | *b.d.l. | 2.4 ± 0.8 | 1.4 ± 1.0 |
| 9.0 - 9.6 m | *b.d.l. | 2.0 ± 1.8 | 0.32 ± 0.08 |
| 10.9 - 11.7 m | *b.d.l. | 0.8 ± 0.4 | 3.3 ± 0.7 |

*b.d.l. = below detection limit of $5.1x10^3$ copies $g^{-1}$

¥n.d. = not determined

**Supplementary Table S3:** Duration of elevated $CO_2$ and $CH_4$ production (in days) at the beginning of the main experiment and surplus amount of $CO_2$ and $CH_4$ produced during the phase of elevated $CO_2$ and $CH_4$ production rates.

| Sampling site | Depth range (m) | Duration of elevated $CO_2$ and $CH_4$ production (d) | | | Surplus gas production (% of total production) | | |
|---|---|---|---|---|---|---|---|
| | | $CO_2$ aerobic | $CO_2$ anaerobic | $CH_4$ anaerobic | $CO_2$ aerobic | $CO_2$ anaerobic | $CH_4$ anaerobic |
| Samoylov | | | | | | | |
| | 0.6-0.8 | 35±0 | 17±5 | 52±15 | 6.7±1.8 | 8.9±2.1 | 6.8±1.9 |
| | 0.8-1.0 | 35±0 | 14±0 | 62±0 | 4.7±1.1 | 3.7±2.7 | 4.4±0.58 |
| | 1.4-1.6 | 40±4 | 16±4 | 57±7 | 5.5±1.5 | 4.4±0.44 | 5.7±0.92 |
| | 1.9-2.1 | 35±0 | 13±0 | 61±0 | 5.5±1.4 | 6.0±1.0 | 9.4±1.6 |
| | 2.8-3.1 | 30±4 | 25±8 | 61±0 | 8.6±0.57 | 20.9±4.6 | 10.8±1.0 |
| | 3.2-3.4 | 35±0 | 21±0 | 61±0 | 9.3±1.2 | 20.3±3.3 | 15.5±1.6 |
| Kurungnakh | | | | | | | |
| | 0.7-0.8 | 34±0 | 44±47 | 81±81 | 3.4±0.16 | 3.4±1.3 | 8.0±11.1 |
| | 0.9-1.1 | 29±5 | 13±0 | 6±9 | 4.0±0.76 | 6.6±0.47 | 0.46±0.66 |
| | 1.2-1.3 | 35±0 | 13±0 | #n.i. | 12.3±4.1 | 3.6±0.57 | #n.i. |
| | 3.1-3.3 | 35±0 | 22±0 | 11±16 | 14.8±3.3 | 26.6±1.6 | 0.4±0.57 |
| | 3.6-3.8 | 42±0 | 26±8 | #n.i. | 19.1±2.9 | 27.3±0.69 | #n.i. |
| | 4.1-4.3 | 35±0 | 31±8 | 22±0 | 10.6±0.93 | 28.3±14.9 | 7.7±3.4 |
| Mean ± SD | | 35±3 | 21±9 | 40±29 | 8.7±4.8 | 13.3±10.4 | 5.8±5.0 |

#n.i. = no increase

**Supplementary Table S4:** Total amount of $CO_2$ and $CH_4$ production normalized to g dry weight of soil (µmol $g^{-1}$) and relative mineralization of permafrost organic carbon to $CO_2$-C (g $CO_2$-C $kgC^{-1}$), $CH_4$-C (g $CH_4$-C $kgC^{-1}$) and $CO_2$-C equivalents (g $CO_2$-C-eq. $kgC^{-1}$) under oxic and anoxic incubation conditions during the three years' incubation period of the main experiment. The production of anoxic $CO_2$-C equivalents were calculated using a GWP of 28 for $CH_4$ corrected for different weights of $CO_2$ and $CH_4$ (ref 9). Presented are mean values of three replicates with one standard deviation.

| | total gas production | | | | | relative mineralization of organic carbon | | | | |
|---|---|---|---|---|---|---|---|---|---|---|
| | oxic $CO_2$ | anoxic $CO_2$ | $CH_4$ | ratio oxic/anoxic | ratio $CO_2/CH_4$ | oxic $CO_2$-C | anoxic $CO_2$-C | $CH_4$-C | $CO_2$-C-eq. | ratio anoxic/oxic |
| Sample | µmol $g^{-1}$ | | | | | g $CO_2$-C $kgC^{-1}$ | g $CO_2$-C $kgC^{-1}$ | g $CH_4$-C $kgC^{-1}$ | g $CO_2$-C-eq. $kgC^{-1}$ | $CO_2$-C-eq. |
| Samoylov | | | | | | | | | | |
| 0.6-0.8 m | 19.5 ± 4.2 | 3.0 ± 0.9 | 3.5 ± 1.5 | 3.0 | 0.87 ± 0.02 | 39 ± 8.4 | 6.1 ± 1.7 | 7.1 ± 2.1 | 78 ± 23 | 2.0 |
| 0.8-1.0 m | 34.7 ± 2.4 | 6.8 ± 0.8 | 6.7 ± 0.5 | 2.6 | 1.01 ± 0.05 | 30 ± 2.1 | 5.9 ± 0.7 | 5.8 ± 0.4 | 65 ± 5.1 | 2.2 |
| 1.4-1.6 m | 111 ± 16.7 | 21.8 ± 5.2 | 22.5 ± 6.4 | 2.5 | 0.98 ± 0.07 | 29 ± 4.4 | 5.7 ± 1.3 | 5.9 ± 1.7 | 66 ± 18 | 2.3 |
| 1.9-2.1 m | 66.9 ± 9.0 | 10.4 ± 1.9 | 11.2 ± 2.1 | 3.1 | 0.93 ± 0.01 | 18 ± 2.5 | 2.9 ± 0.5 | 3.1 ± 0.6 | 34 ± 6.3 | 1.9 |
| 2.8-3.1 m | 48.1 ± 5.2 | 7.3 ± 0.7 | 7.8 ± 1.0 | 3.2 | 0.94 ± 0.04 | 12 ± 1.3 | 1.8 ± 0.2 | 1.9 ± 0.2 | 22 ± 2.6 | 1.8 |
| 3.2-3.4 m | 61.3 ± 3.5 | 5.7 ± 0.2 | 5.8 ± 0.1 | 5.4 | 0.98 ± 0.06 | 18 ± 1.0 | 1.7 ± 0.1 | 1.7 ± 0.0 | 19 ± 0.3 | 1.1 |
| Kurungnakh | | | | | | | | | | |
| 0.7-0.8 m | 52.7 ± 0.5 | 7.3 ± 1.6 | 6.5 ± 1.1 | 3.8 | 1.13 ± 0.06 | 16 ± 0.2 | 2.3 ± 0.5 | 2.0 ± 0.3 | 23 ± 4.0 | 1.4 |
| 0.9-1.1 m | 158 ± 23.0 | 20.9 ± 2.6 | 23.7 ± 5.2 | 3.5 | 0.90 ± 0.12 | 15 ± 2.2 | 2.0 ± 0.3 | 2.3 ± 0.5 | 25 ± 5.4 | 1.7 |
| 1.2-1.3 m | 36.1 ± 9.1 | 13.6 ± 1.1 | 13.2 ± 1.4 | 1.3 | 1.03 ± 0.03 | 5.9 ± 1.5 | 2.2 ± 0.2 | 2.2 ± 0.2 | 24 ± 2.5 | 4.1 |
| 3.1-3.3 m | 46.2 ± 3.4 | 10.9 ± 0.8 | 15.2 ± 4.0 | 1.8 | 0.76 ± 0.20 | 16 ± 1.1 | 3.7 ± 0.3 | 5.1 ± 1.4 | 56 ± 14 | 3.6 |
| 3.6-3.8 m | 29.1 ± 0.5 | 6.3 ± 0.8 | 13.5 ± 2.4 | 1.5 | 0.48 ± 0.11 | 9.3 ± 0.2 | 2.0 ± 0.3 | 4.3 ± 0.8 | 46 ± 8.0 | 4.9 |
| 4.1-4.3 m | 56.3 ± 11.2 | 7.3 ± 0.3 | 6.8 ± 0.4 | 4.0 | 1.07 ± 0.01 | 14 ± 2.8 | 1.8 ± 0.1 | 1.7 ± 0.1 | 19 ± 1.0 | 1.4 |
| mean ± SD | 60.0 ± 38.6 | 10.1 ± 5.9 | 11.4 ± 6.6 | 3.0 ± 1.2 | 0.92 ± 0.18 | 19 ± 9.6 | 3.2 ± 1.7 | 3.6 ± 1.9 | 40 ± 21 | 2.3 ± 1.2 |

**Supplementary Table S5:** Total amount of $CO_2$ and $CH_4$ production normalized to g dry weight of soil (µmol $g^{-1}$) and relative mineralization of permafrost organic carbon to $CO_2$-C (g $CO_2$-C $kgC^{-1}$), $CH_4$-C (g $CH_4$-C $kgC^{-1}$) and $CO_2$-C equivalents (g $CO_2$-C-eq. $kgC^{-1}$) under oxic and anoxic incubation conditions predicted by the calibrated organic carbon decomposition model until 2100. The production of anoxic $CO_2$-C equivalents were calculated using a GWP of 28 for $CH_4$ corrected for different weights of $CO_2$ and $CH_4$ (ref 9). Presented are mean values of three replicates with one standard deviation.

| | total gas production | | | | | relative mineralization of organic carbon | | | | |
|---|---|---|---|---|---|---|---|---|---|---|
| | oxic $CO_2$ | anoxic $CO_2$ | $CH_4$ | ratio oxic/anoxic | ratio $CO_2/CH_4$ | oxic $CO_2$-C | anoxic $CO_2$-C | $CH_4$-C | $CO_2$-C-equiv. | ratio anoxic/oxic |
| Sample | µmol g-1 | | | | | g $CO_2$-C $kgC^{-1}$ | g $CO_2$-C $kgC^{-1}$ | g $CH_4$-C $kgC^{-1}$ | g $CO_2$-C-eq. $kgC^{-1}$ | $CO_2$-C-eq. |
| Samoylov | | | | | | | | | | |
| 0.6-0.8 m | 113 ± 26 | 14.9 ± 5.5 | 21.9 ± 7.3 | 3.1 | 0.68 ± 0.03 | 228 ± 52 | 30 ± 11 | 44 ± 15 | 479± 160.4 | 2.1 |
| 0.8-1.0 m | 211 ± 22 | 37.2 ± 5.3 | 46.0 ± 4.3 | 2.5 | 0.81 ± 0.04 | 183 ± 19 | 32 ± 4.6 | 40 ± 3.7 | 438 ± 42.6 | 2.4 |
| 1.4-1.6 m | 683 ± 110 | 119 ± 37 | 158 ± 54 | 2.5 | 0.76 ± 0.07 | 178 ± 29 | 31 ± 9.7 | 41 ± 14 | 451 ± 152 | 2.5 |
| 1.9-2.1 m | 422 ± 63 | 50.1 ± 12 | 74.5 ± 12 | 3.4 | 0.67 ± 0.05 | 116 ± 17 | 14 ± 3.2 | 20 ± 3.3 | 222 ± 36.8 | 1.9 |
| 2.8-3.1 m | 286 ± 30 | 36.1 ± 3.8 | 44.7 ± 8.0 | 3.5 | 0.81 ± 0.06 | 71 ± 8 | 9 ± 0.9 | 11 ± 2.0 | 122 ± 1.2 | 1.7 |
| 3.2-3.4 m | 363 ± 21 | 24.8 ± 2.1 | 34.0 ± 1.0 | 6.2 | 0.73 ± 0.08 | 108 ± 6 | 7 ± 0.6 | 10 ± 0.3 | 110 ± 3.7 | 1.0 |
| Kurungnakh | | | | | | | | | | |
| 0.7-0.8 m | 398 ± 77 | 42.9 ± 11 | 46.5 ± 11 | 4.5 | 0.92 ± 0.09 | 123 ± 24 | 13 ± 3.4 | 14 ± 3.3 | 160± 37.2 | 1.3 |
| 0.9-1.1 m | 1015 ± 173 | 103 ± 12 | 157 ± 31 | 3.9 | 0.66 ± 0.05 | 98 ± 17 | 10 ± 1.2 | 15 ± 3.1 | 165 ± 32.2 | 1.7 |
| 1.2-1.3 m | 211 ± 46 | 77.2 ± 6.7 | 95.0 ± 22 | 1.2 | 0.83 ± 0.12 | 34 ± 8 | 13 ± 1.1 | 16 ± 3.6 | 171 ± 38.2 | 4.9 |
| 3.1-3.3 m | 253 ± 26 | 64.7 ± 3.0 | 69.1 ± 3 | 1.9 | 0.95 ± 0.13 | 85 ± 9 | 22 ± 1.0 | 23 ± 4.2 | 258 ± 43.8 | 3.0 |
| 3.6-3.8 m | 158 ± 12 | 37.6 ± 18 | 64.5 ± 22 | 1.5 | 0.59 ± 0.28 | 50 ± 4 | 12 ± 5.7 | 21 ± 7.0 | 221 ± 77.2 | 4.4 |
| 4.1-4.3 m | 319 ± 78 | 40.9 ± 0.54 | 33.7 ± 2.6 | 4.3 | 1.22 ± 0.08 | 79 ± 19 | 10 ± 0.1 | 8.3 ± 0.6 | 94.6 ± 6.7 | 1.2 |
| mean ± SD | 369 ± 253 | 54.0 ± 31 | 70.4 ± 45 | 3.0 ± 1.2 | 0.80 ± 0.17 | 113 ± 58 | 17 ± 9.3 | 22 ± 13 | 241 ± 138 | 2.4 ± 1.2 |

**Supplementary Table S6:** Projected thaw of permafrost organic carbon and formation of $CO_2$ and $CH_4$ (mean ± SD) in unsaturated (oxic) and saturated (anoxic) soils until 2100 at the pan-Arctic scale under representative concentration pathways (RCP) 4.5 and 8.5.

| | RCP 4.5 | | RCP 8.5 | |
|---|---|---|---|---|
| | oxic/non-saturated | anoxic/saturated | oxic/non-saturated | anoxic/saturated |
| ‡organic carbon thaw (Pg C) | 47.6 ± 46.7 | 19.2 ± 23.4 | 172.4 ± 79.0 | 70.4 ± 48.1 |
| $CO_2$ produced until 2100 (Pg $CO_2$-C) | 2.6 ± 3.2 | 0.17 ± 0.26 | 9.5 ± 7.0 | 0.62 ± 0.61 |
| $CH_4$ produced until 2100 (Pg $CH_4$-C) | - | 0.22 ± 0.34 | - | 0.82 ± 0.81 |
| Sum organic carbon mineralization (Pg C) | 2.6 ± 3.2 | 0.39 ± 0.60 | 9.5 ± 7.0 | 1.4 ± 1.4 |
| ¥Sum $CO_2$-C equivalent production (Pg) | 2.6 ± 3.2 | 2.4 ± 3.7 | 9.5 ± 7.0 | 8.9 ± 8.8 |
| Total C mineralization (Pg) | 3.0 ± 3.6 | | 11.0 ± 7.5 | |
| Total $CO_2$-C equivalent production (Pg) | 5.1 ± 5.9 | | 18.5 ± 12.1 | |

‡fraction of saturated : unsaturated soils from ref 2

¥based on a GWP of 28 (ref 9), corrected for weight differences between $CH_4$ and $CO_2$

**Supplementary References:**


1. Koven CD, Schuur EAG, Schädel C, Bohn TJ, Burke EJ, Chen G*, et al.* A simplified, data-constrained approach to estimate the permafrost carbon–climate feedback. *Philosophical Transactions of the Royal Society A: Mathematical, Physical and Engineering Sciences* 2015, **373**(2054).

2. Harden JW, Koven CD, Ping C-L, Hugelius G, McGuire AD, Camill P*, et al.* Field information links permafrost carbon to physical vulnerabilities of thawing. *Geophysical Research Letters* 2012, **39**(15).

3. Hugelius G, Strauss J, Zubrzycki S, Harden JW, Schuur EAG, Ping C-L*, et al.* Estimated stocks of circumpolar permafrost carbon with quantified uncertainty ranges and identified data gaps. *Biogeosciences* 2014, **11**(23)**:** 6573-6593.

4. Schädel C, Schuur EAG, Bracho R, Elberling B, Knoblauch C, Lee H*, et al.* Circumpolar assessment of permafrost C quality and its vulnerability over time using long-term incubation data. *Global Change Biology* 2014, **20**(2)**:** 641-652.

5. Cooper MDA, Estop-Aragones C, Fisher JP, Thierry A, Garnett MH, Charman DJ*, et al.* Limited contribution of permafrost carbon to methane release from thawing peatlands. *Nature Clim Change* 2017, **7**(7)**:** 507-511.

6. Schuur EAG, McGuire AD, Schädel C, Grosse G, Harden JW, Hayes DJ*, et al.* Climate change and the permafrost carbon feedback. *Nature* 2015, **520**(7546)**:** 171-179.

7. Knoblauch C, Beer C, Sosnin A, Wagner D, Pfeiffer E-M. Predicting long-term carbon mineralization and trace gas production from thawing permafrost of Northeast Siberia. *Global Change Biology* 2013, **19**(4)**:** 1160-1172.

8. IUSS Working Group WRB. *World Reference Base for Soil Resources 2014 International soil classification system for naming soils and creating legends for soil maps*, vol. 106. FAO: Rome, 2014.

9. Myhre G, Shindell D, Bréon F-M, Collins W, Fuglestvedt J, Huang J*, et al.* Anthropogenic and Natural Radiative Forcing. In: Stocker TF, Qin D, Plattner G-K, Tignor M, Allen SK, Boschung J*, et al.* (eds). *Climate Change 2013: The Physical Science Basis. Contribution of Working Group I to the Fifth Assessment Report of the Intergovernmental Panel on Climate Change*. Cambridge University Press: Cambridge, United Kingdom and New York, USA, 2013, pp 659-740.